Supporting Information

A transformable gold nanocluster aggregates-based synergistic strategy for potentiated radiation/gene therapy of cancer

Chun Wu,[a] Xuancheng Du,[b] Bingqing Jia,[b] Chengmei Zhang,[c] Weifeng Li,[b] Tian-Cai Liu,[d] and Yong-Qiang Li[*b,e]*

[a] State Key Laboratory of Radiation Medicine and Protection, School of Radiation Medicine and Protection, Soochow University, Suzhou 215123, China.

[b] Institute of Advanced Interdisciplinary Science, School of Physics, Shandong University, Jinan 250100, China.

[c] Laboratory Animal Center of Shandong University, Jinan 250012, China.

[d] Key Laboratory of Antibody Engineering of Guangdong Higher Education Institutes, School of Laboratory Medicine and Biotechnology, Southern Medical University, Guangzhou 510515, China.

[e] Suzhou Research Institute, Shandong University, Suzhou 215123, China.

* Corresponding authors: yqli@sdu.edu.cn (Y.-Q. Li)

Supporting Figures

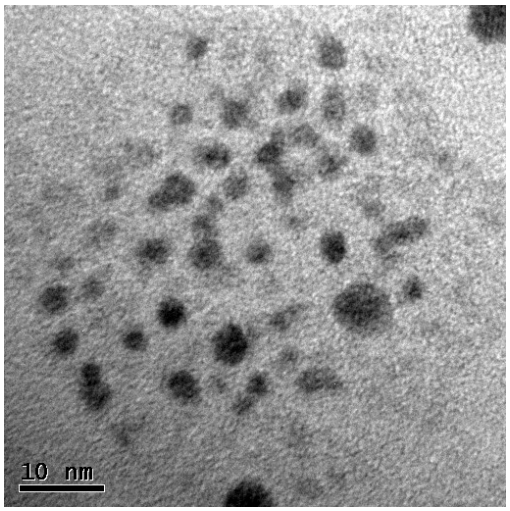

Figure S1. TEM image of AuNC.

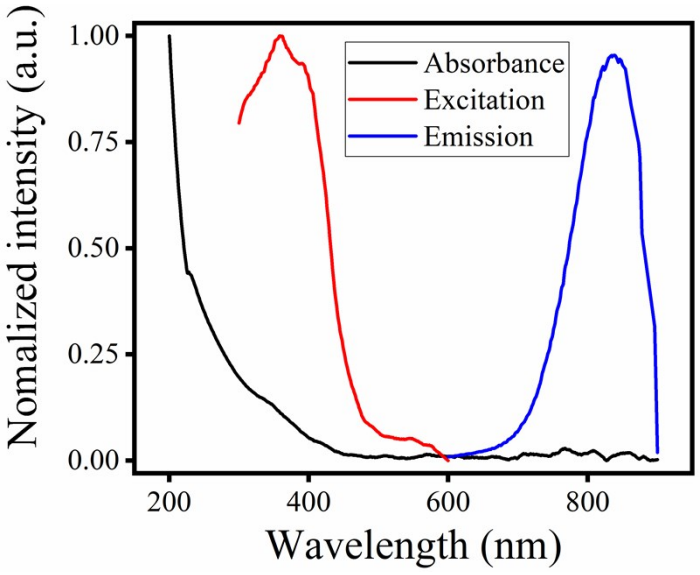

Figure S2. Absorption, excitation and fluorescence emission spectra of AuNC.

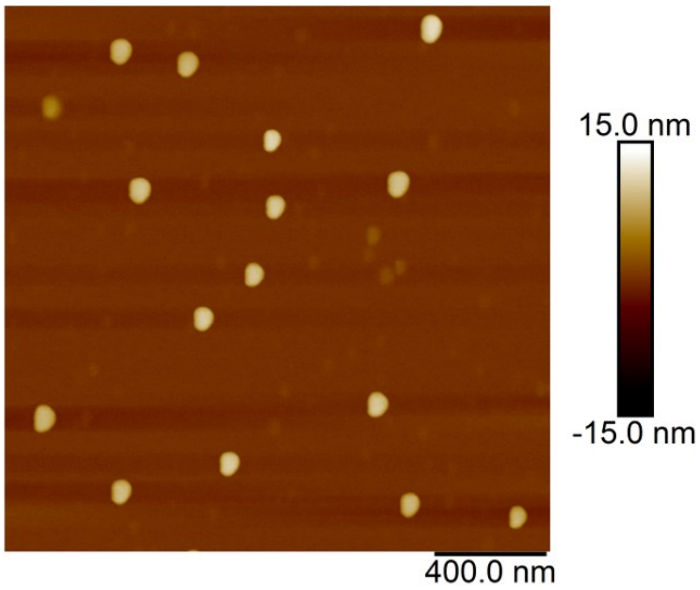

Figure S3. Typical atomic force microscopy (AFM) image of AuNC.

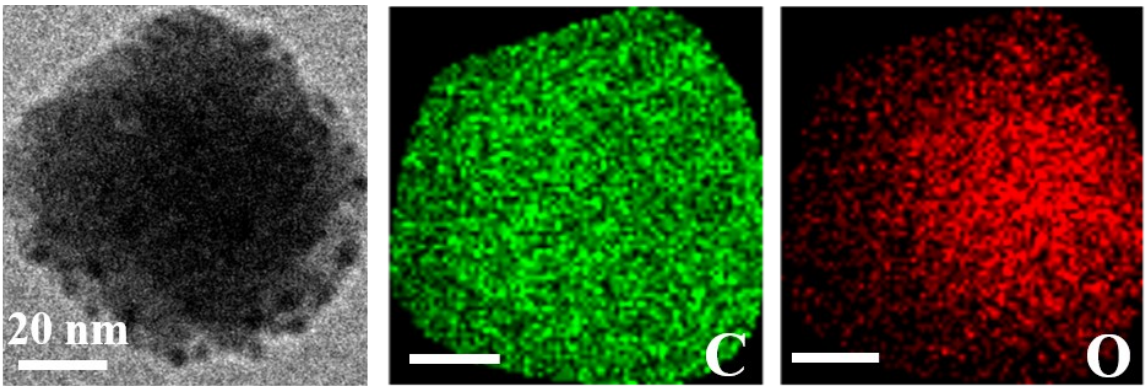

Figure S4. High-angle annular dark field scanning TEM image and corresponding energy-dispersive X-ray (EDX) mapping of AuNC-ASON. The microscope field is the same as Figure 1c.

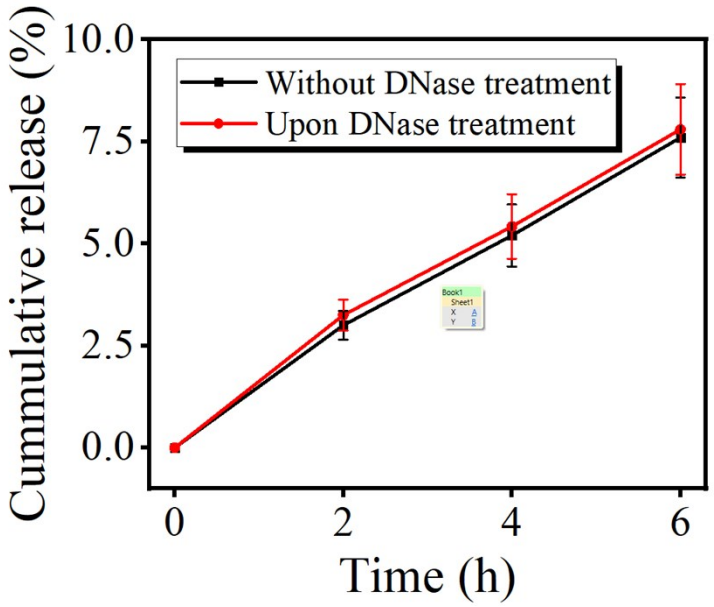

Figure S5. Release curves of ASON loaded in AuNC-ASON with and without DNase treatment. The values of ASON cumulative release rate represent the mean of three independent experiments, and the error bars indicate the standard deviation (SD) from the mean.

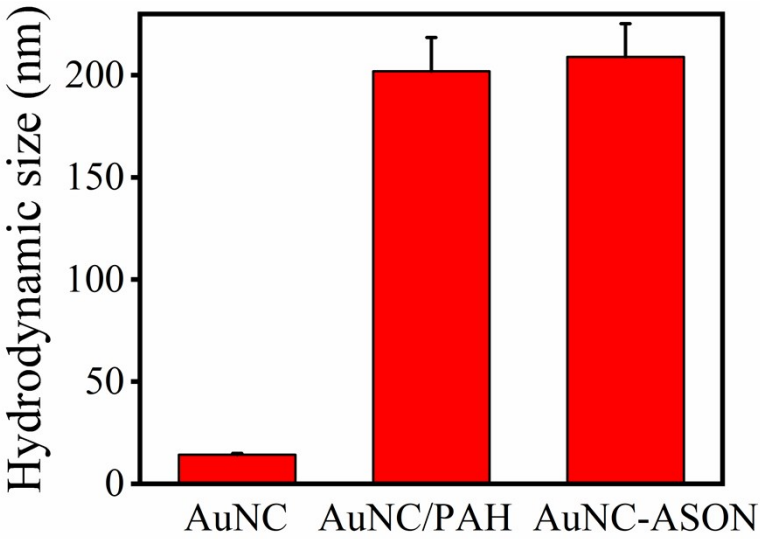

Figure S6. Hydrodynamic sizes of AuNC, AuNC/PAH, and AuNC-ASON in DI water. The values of hydrodynamic size represent the mean of three independent experiments, and the error bars indicate the SD from the mean.

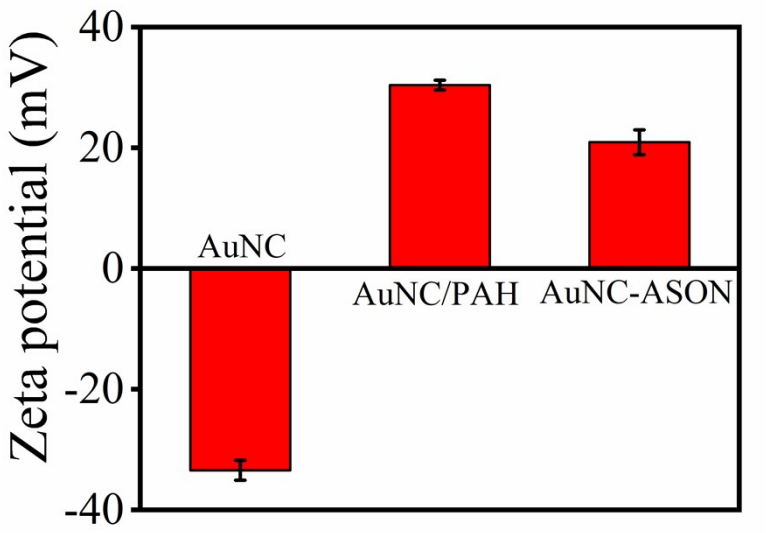

Figure S7. Zeta potentials of AuNC, AuNC/PAH, and AuNC-ASON water solutions. The values of zeta potential represent the mean of three independent experiments, and the error bars indicate the SD from the mean.

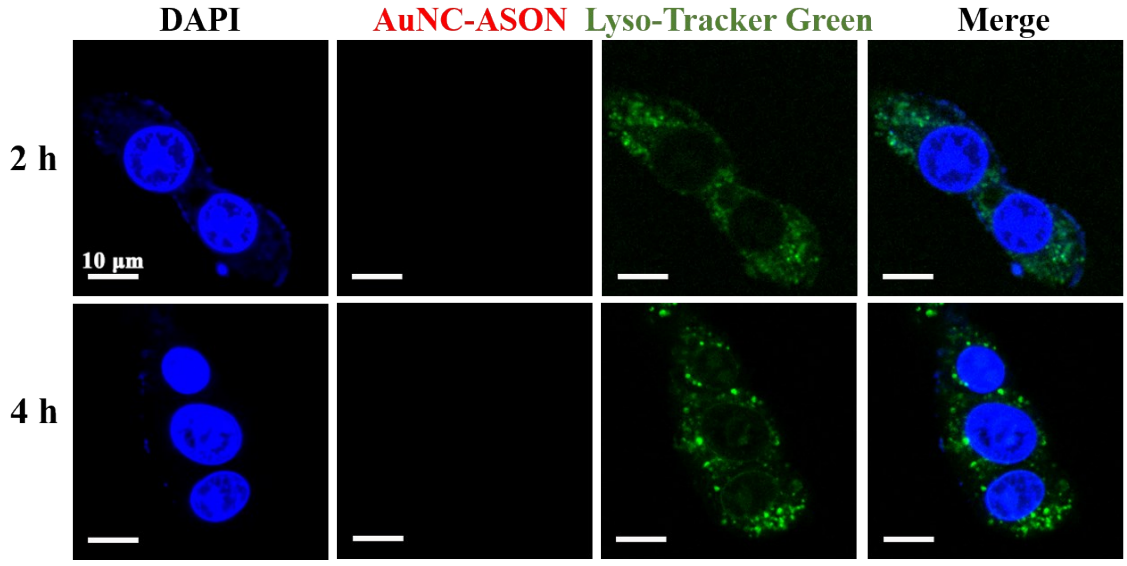

Figure S8. Representative CLFM images of 4T1 cells after incubation with AuNC-ASON for 2 and 4 h, respectively, to investigate the endosome/lysosome escape of AuNC-ASON. Here LysoTracker green was used as a fluorescent dye to label intracellular endosome and lysosomes.

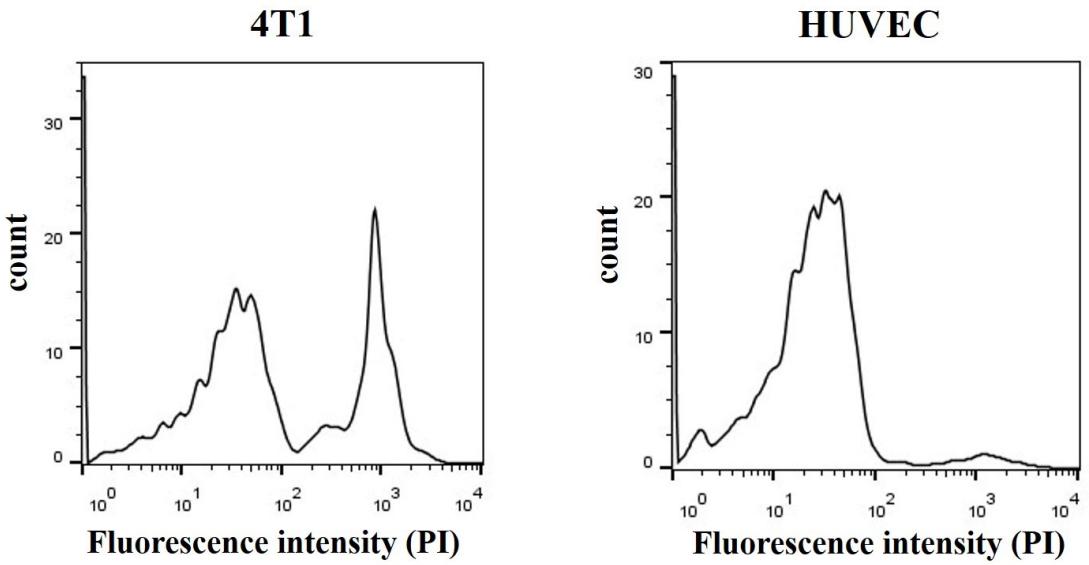

Figure S9. Histogram shows the fluorescence intensity of PI (staining dead cells) measured by flow cytometry in the 4T1 cells after incubation with AuNC-ASON (25 μg/mL of AuNC) for 24 h.

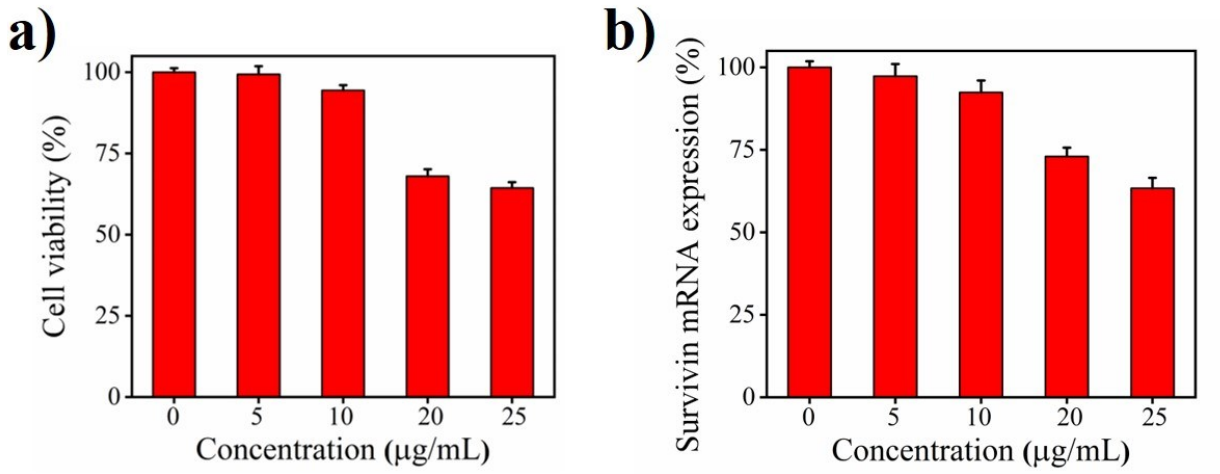

Figure S10. The viability (a) and survivin mRNA expression (b) of 4T1 cells after incubation with the AuNC-ASON with different AuNC concentrations for 24 h. The values of cell viability and survivin mRNA expression represent the mean of three independent experiments, and the error bars indicate the SD from the mean.

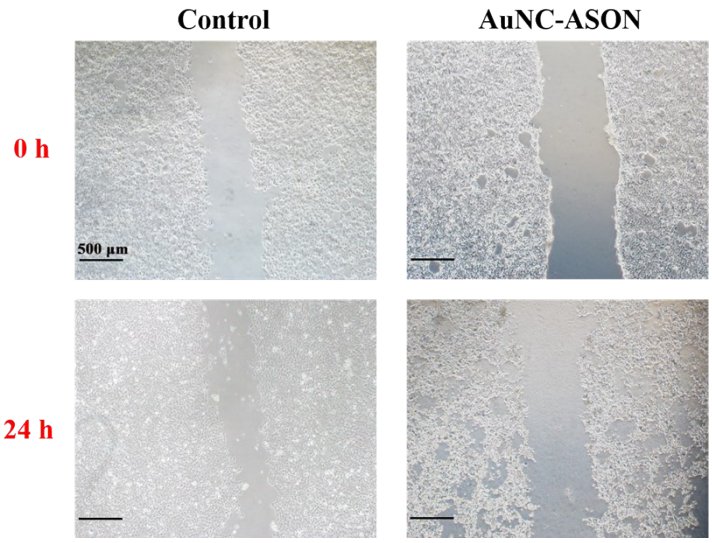

Figure S11. Scratch assay of 4T1 cells incubated with AuNC-ASON (25 μg/mL of AuNC) for 24 h. The 4T1 cells without any treatment were used as the control.

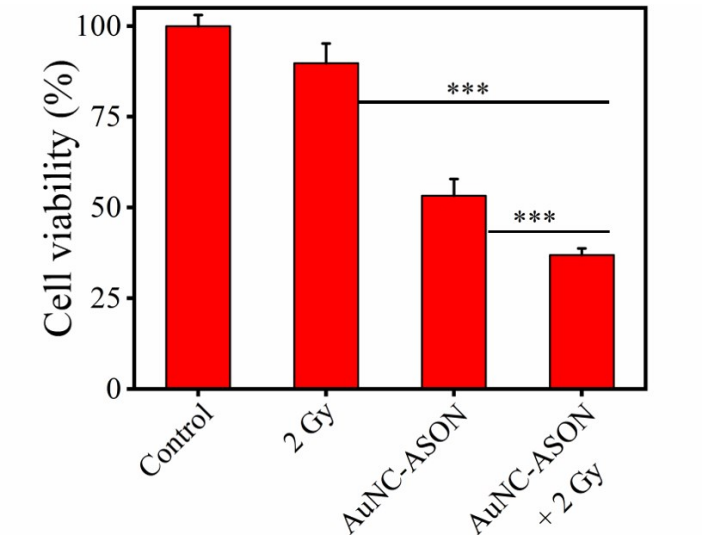

Figure S12. The viability of 4T1 cells in four different treatment groups. The 4T1 cells without any treatment were used as the control. The values of cell viability represent the mean of three independent experiments, and the error bars indicate the SD from the mean. *** indicates $P < 0.001$.

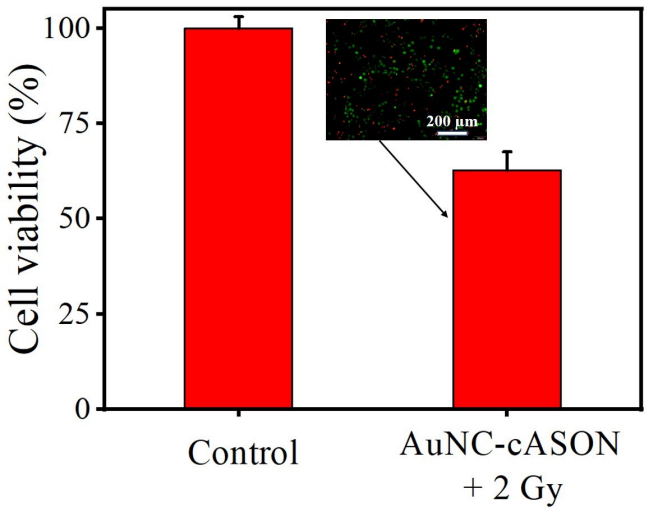

Figure S13. The cell viability and corresponding live/dead cell staining of 4T1 cells in the condition of AuNC-cASON plus radiation (AuNC-cASON + 2 Gy). The 4T1 cells without any treatment were used as the control. The values of cell viability represent the mean of three independent experiments, and the error bars indicate the SD from the mean.

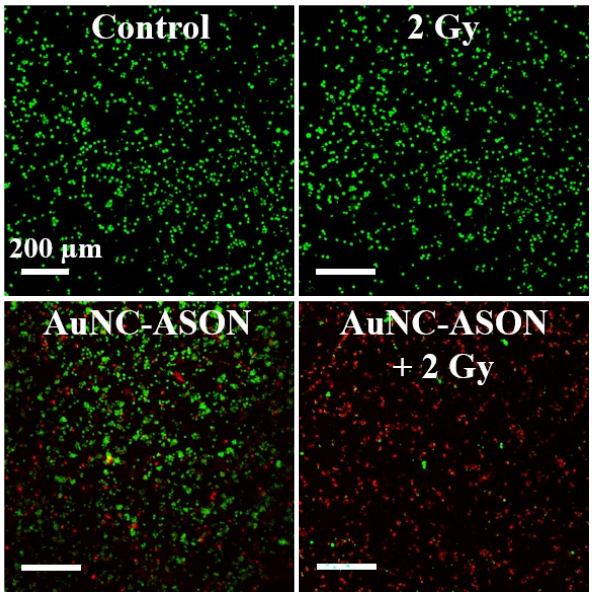

Figure S14. Typical overlapping live/dead staining images for 4T1 cells in four treatment groups. The 4T1 cells without any treatment were used as the control.

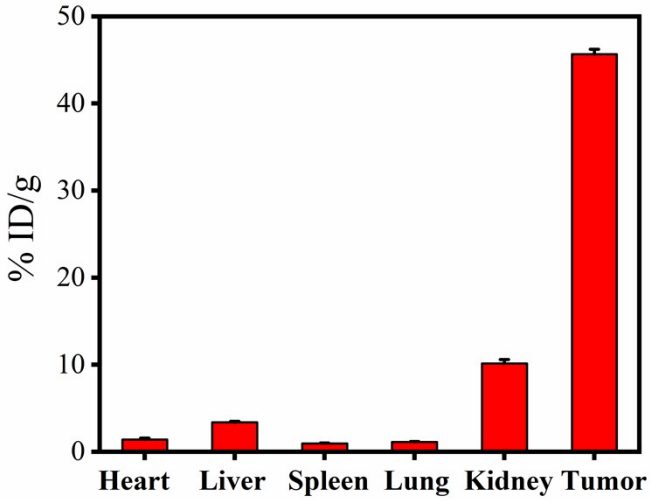

Figure S15. Biodistribution of Au content in 4T1 tumor-bearing mice intratumorally injected with AuNC-ASON at the 3rd day postinjection. The values for Au content are means ± SD of 3 mice from three independent experiments.

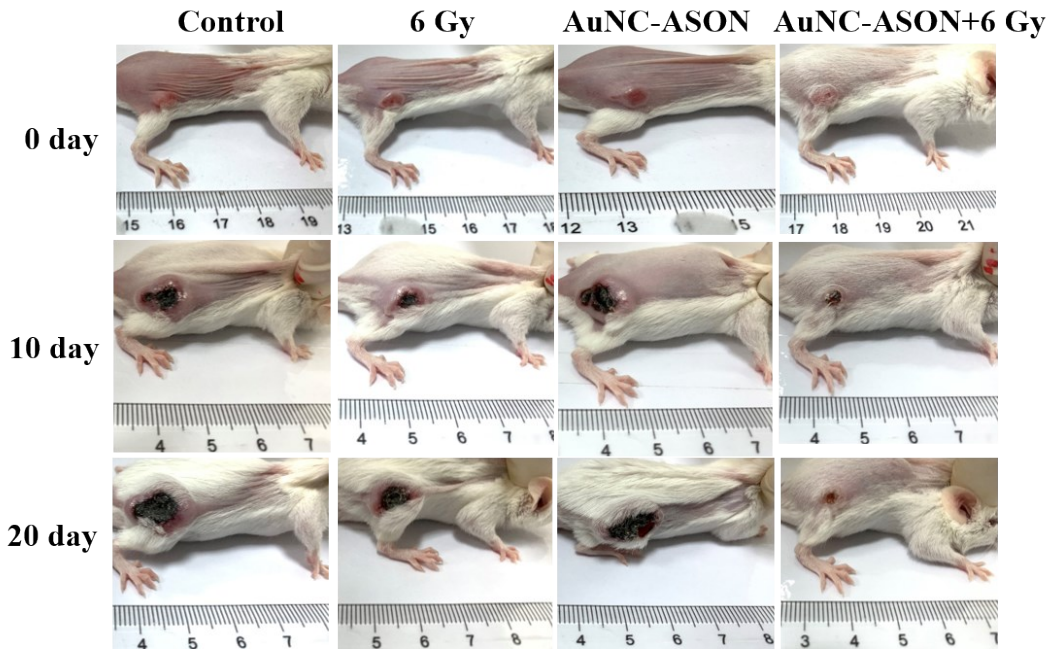

Figure S16. Representative photographs of the 4T1 tumor-bearing mice within 20 days postinjection in four different treatment groups.

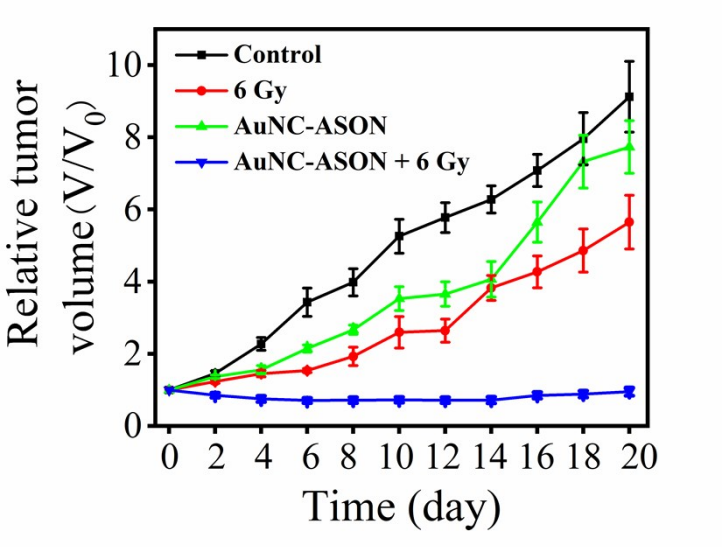

Figure S17. The growth curves of 4T1 tumor relative volume in the four different treatment groups. V_0 and V indicate the volume of tumor before and after treatment, respectively. The values of relative tumor volume are means ± SD of 5 mice from three independent experiments.

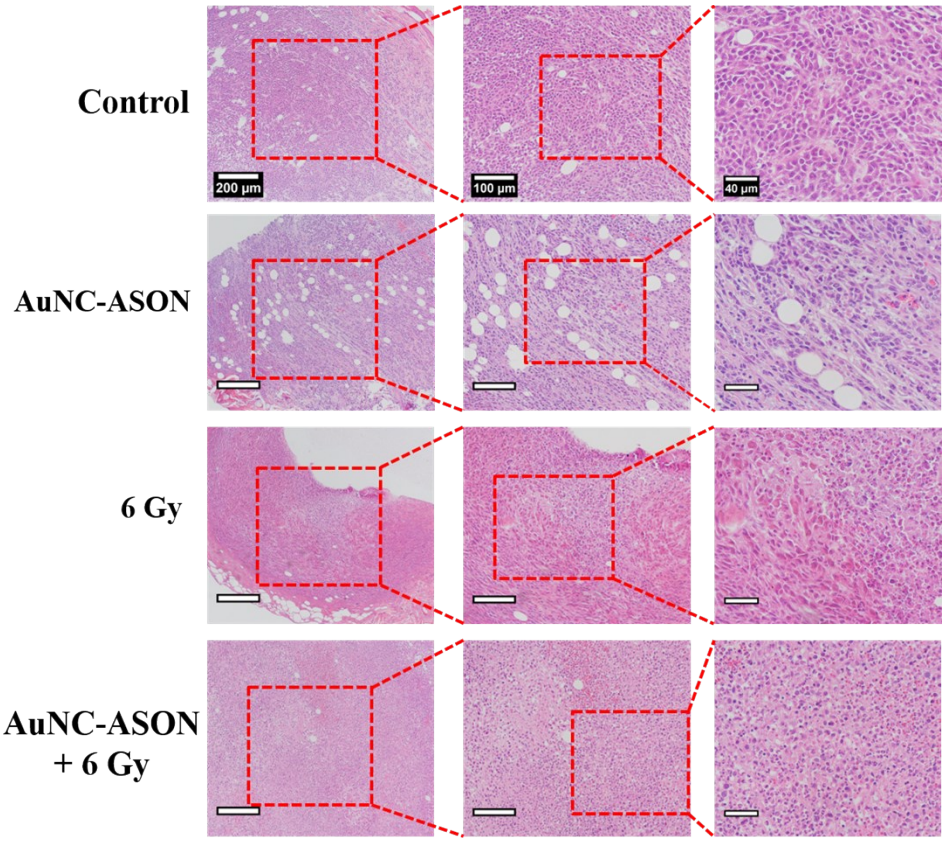

Figure S18. The H&E staining images of tumor tissues of 4T1 tumor-bearing mice after 20 days treatment of control (PBS), 6 Gy, AuNC-ASON, and AuNC-ASON + 6 Gy, respectively.

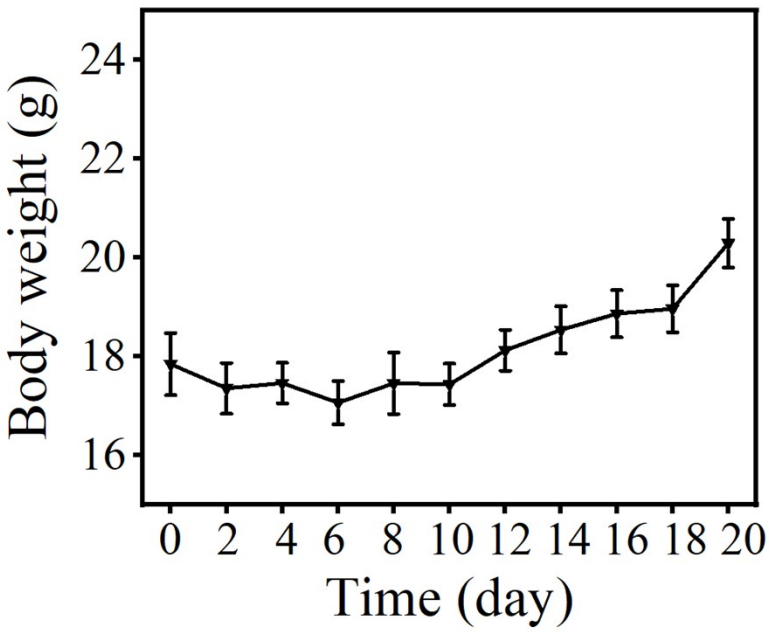

Figure S19. The change of body weight of the 4T1 tumor-bearing mice during 20 days treatment of AuNC-ASON + 6 Gy. The values of tumor body weight are means ± SD of 5 mice from three independent experiments.

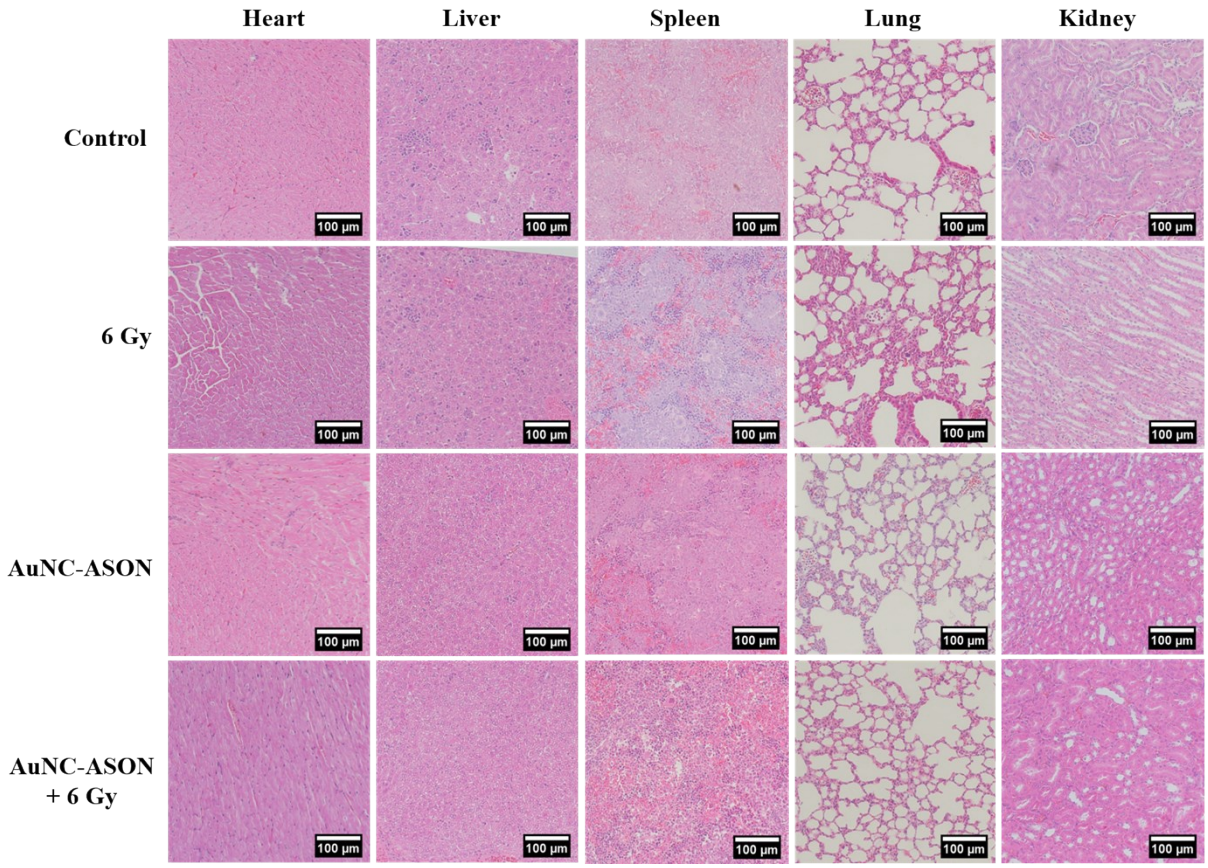

Figure S20. The H&E staining images of different organs of 4T1 tumor-bearing mice after 20 days treatment of control (PBS), 6 Gy, AuNC-ASON, and AuNC-ASON + 6 Gy, respectively.